# pH Dependence of Stability of Staphylococcal Nuclease: Evidence of Substantial Electrostatic Interactions in the Denatured State†

Steven T. Whitten and Bertrand García-Moreno E.*

*Department of Biophysics, Johns Hopkins University, Baltimore, Maryland 21218*

*Received May 4, 2000; Revised Manuscript Received August 11, 2000*

ABSTRACT: The pH dependence of stability of staphylococcal nuclease was studied with two independent equilibrium thermodynamic approaches. First, by measurement of stability in the pH range 9 to 3.5 by fluorescence-monitored denaturation with urea ($\Delta G^{o}_{urea}$), GdnHCl ($\Delta G^{o}_{Gdn}$), and heat ($\Delta G^{o}_{T}$). Second, by numerical integration of $H^+$ titration curves ($\Delta G^{o}_{\Delta\nu}$) measured potentiometrically under native (100 mM KCl) and unfolding (6.0 M GdnHCl) conditions. The pH dependence of stability described by $\Delta G^{o}_{urea}$, $\Delta G^{o}_{Gdn}$, and $\Delta G^{o}_{T}$ was comparable but significantly different from the one described by $\Delta G^{o}_{\Delta\nu}$. The decrease in $\Delta G^{o}_{\Delta\nu}$ between pH 9 and pH 4 was 4 kcal/mol greater than the decrease in $\Delta G^{o}_{urea}$, $\Delta G^{o}_{Gdn}$, and $\Delta G^{o}_{T}$ in the same pH range. In 6 M GdnHCl, all the ionizable groups titrated with the p$K_a$ values of model compounds. Therefore, $\Delta G^{o}_{\Delta\nu}$ represents the free energy difference between the native state (N) and an ensemble of unstructured, or expanded, and highly screened conformations. In contrast, the shallower pH dependence of stability described by $\Delta G^{o}_{urea}$ and by $\Delta G^{o}_{T}$ between pH 9 and 5 was consistent with the titration of histidines with depressed, nativelike p$K_a$ values in the denatured state (D). These depressed p$K_a$ values likely reflect long-range electrostatic interactions with the other 29 basic groups and are a consequence of the compact character of the D state. The steep change in $\Delta G^{o}_{urea}$ and $\Delta G^{o}_{T}$ at pH < 5 suggests that near pH 5 the structural and thermodynamic character of the D state shifts toward a state in which acidic residues titrate with normal p$K_a$ values, presumably because the electrostatic interactions with basic residues are lost, maybe as a consequence of an expansion.

The stability of proteins is described most rigorously in terms of free energy differences ($\Delta G°$) between native (N)[1] and denatured (D) states.[2] A goal of quantitative studies of folding and stability of proteins is to determine the magnitude and balance between different noncovalent contributions to stability and to interpret stability in structural terms. This remains a challenging problem, especially since the D states of many proteins are now known to be structured and compact. Under these circumstances, assumptions about the structure of the D state and about its thermodynamic properties and the noncovalent factors that determine them are not necessarily valid. Unfortunately, the structure of D states is difficult to detect and to study in detail. Thermodynamic properties of D states are equally difficult to measure experimentally.

As part of a comprehensive study of the contributions by electrostatic interactions to the stability and folding of proteins, we studied the pH dependence of stability of staphylococcal nuclease (SNase). The pH dependence of stability of proteins is determined by differences in the proton ($H^+$) binding affinity of the N and D states (*1*−*4*). To the degree that p$K_a$ values of ionizable groups in proteins are determined by electrostatic effects, the difference in $H^+$ affinity of N and D states reflects differences in the electrostatic contributions to their free energy. One objective of this study was to assess quantitatively the contributions by electrostatic interactions to the stability of the N state and to the structure and thermodynamic character of the D state.

The pH dependence of stability of proteins is usually studied by measurement of ΔG° by chemical or thermal denaturation over a range of pH values (*5*−*12*). The net difference in the number of $H^+$ bound to the N and D states ($\Delta\nu_{H^+}$) at a given pH can be obtained from the pH dependence of $\Delta G°$. $\Delta\nu_{H^+}$ is necessary but not sufficient to understand the pH dependence of stability in structural terms

† This work was supported by NSF Grant MCB-9600991 to B.G.M.E.

* To whom correspondence should be addressed. Department of Biophysics, Johns Hopkins University, 3400 N. Charles St., Baltimore, MD 21218. Telephone: (410) 516-4497. Fax: (410) 516−4118. E-mail: bertrand@jhu.edu.

[1] Abbreviations: SNase, staphylococcal nuclease; N, native state; GdnHCl, guanidine hydrochloride; D, denatured state populated during thermal or chemical denaturation; U, unfolded state achieved in 6 M GdnHCl; $U_A$, acid-unfolded state; $H^+$, hydrogen ions, protons; $\Delta\nu_{H^+}$, difference in the number of bound $H^+$ in two different states of SNase; $\Delta G^{o}_{\Delta\nu}$, standard free energy difference between U and N states measured by numerical integration of $H^+$ titration curves; $\Delta G^{o}_{urea}$, standard free energy difference between D and N states measured by urea denaturation; $\Delta G^{o}_{Gdn}$, standard free energy difference between D and N states measured by GdnHCl denaturation; $\Delta G^{o}_{T}$, standard free energy difference between D and N states measured by temperature denaturation; $pH_{mid}$, pH at the midpoint of an acid-induced unfolding transition; $T_m$, temperature at the midpoint of a temperature-induced denaturation; CD, circular dichroism; NMR, nuclear magnetic resonance; DSC, differential scanning calorimetry.

[2] The word "state" is used to denote the dynamic ensemble of conformations that are present under native, denaturing, or unfolding conditions.

10.1021/bi001015c CCC: $19.00 
Published on Web 10/21/2000

or to infer the $H^+$ titration behavior of the D state. The $H^+$ titration properties of the N state are also needed to provide a point of reference. For example, $H^+$ titration properties of D states of barnase (*5*, *6*), chymotrypsin inhibitor 2 (*7*), and ovomucoid third domain (*13*) were deduced by analysis of both the $\Delta\nu_{H^+}$ obtained from the pH dependence of $\Delta G°$ and the $H^+$ titration properties of the N state obtained from p$K_a$ values of individual groups measured by NMR spectroscopy.

In these proteins, the p$K_a$ values of some acidic residues in the D states were found to be depressed relative to the p$K_a$ values of model compounds in water. These depressed p$K_a$ values signal the presence of stabilizing electrostatic interactions between acidic and basic residues in the D state at the low pH values where the p$K_a$ values were measured. In the case of the N terminal domain of the L9 protein, it was even possible to show that the p$K_a$ values of acidic residues were depressed in the peptide fragments designed to mimic the D state of that protein in water (*14*). In structure-based calculations of the pH dependence of stability of proteins, the underlying assumption is that the p$K_a$ values of ionizable groups in the D state are those of model compounds in water (*1*, *4*). Evidently, this assumption is not valid for some proteins.

Our interest in SNase stems precisely from the fact that the D states that are populated during heat (*15*), GdnHCl (*16*), urea (*17*), and acid (*18*, *19*) denaturation of this protein are thought to be structured and compact. SNase is a highly basic protein that contains 33 basic groups and only 28 acidic ones, 7 of which are tyrosines. Its isoionic point is >10. This protein has a high number of positive charges over a wide range of pH. Electrostatic interactions in the D state are likely to be substantial when it is both compact and highly charged, as in the case of SNase.

Quantitative studies of electrostatic effects in the D states of SNase were pursued for three reasons. First, it was of interest to establish the magnitude of the contribution by electrostatics to thermodynamic properties and to the compact character of the D state. Improved understanding of the molecular origins of stability and structure in compact D states of proteins is essential for understanding the folding reaction. Second, it was of interest to establish if the measurement of $H^+$ binding properties of the D state could be harnessed to probe the presence of compactness. Third, assessment of the $H^+$ binding properties of the D state was necessary to understand how electrostatic interactions contribute to the stability of the N state.

When strong electrostatic interactions are present in the D state, the contributions by electrostatics to the stability of the N state cannot be understood without knowledge of the proton-linked thermodynamic properties of the D state. In these cases, it is not valid to assume that the ionizable groups in the D state titrate with the p$K_a$ values of model compounds. Unfortunately, proton-linked thermodynamic properties of the D state cannot be studied with standard experimental approaches because, in general, this state appears unfolded by all useful probes for monitoring conformational transformations (CD, fluorescence, $\Delta C_p$). In the case of SNase, it was not even possible to deduce the $H^+$ titration of the D state from the difference between $\Delta\nu_{H^+}$ obtained from the pH dependence of $\Delta G°$ and the $H^+$ titration of the N state described from p$K_a$s of acidic residues by NMR spectroscopy. These p$K_a$ values cannot be measured in the wild-type protein because the midpoint of the acid unfolding transition of SNase is very close to the normal p$K_a$ of Glu and Asp.

Instead, in this study the $H^+$ titration behavior of the D state of SNase was established by comparing the pH dependence of global stability determined with equilibrium unfolding experiments, with the pH dependence of stability obtained by numerical integration of $H^+$ titration curves measured with direct potentiometric methods for native and unfolded SNase. Specifically, the pH dependence of stability was determined by measurement of unfolding free energies in the pH range 9 to 3.5 by fluorescence-monitored denaturation with urea ($\Delta G°_{urea}$), GdnHCl ($\Delta G°_{Gdn}$), and heat ($\Delta G°_T$). The pH dependence of $\Delta G°_{urea}$, $\Delta G°_{Gdn}$, and $\Delta G°_T$ were compared with each other to determine if the measured energetics were sensitive to the specific denaturant used. The pH dependence of stability was also measured by numerical integration of the difference between $H^+$ titration curves ($\Delta G°_{\Delta\nu}$) measured potentiometrically in 100 mM KCl and in concentrations of GdnHCl much higher than those needed to denature SNase. These potentiometric $H^+$ titration curves constitute the reference behavior that is essential for the interpretation of the pH dependence of stability described by $\Delta G°_{urea}$ or $\Delta G°_T$ in terms of $H^+$ titration properties of the D state.

Previously, Bolen and co-workers tested the validity of $\Delta G°$ values measured by chemical denaturation for several protein by comparing the pH dependence of stability measured by thermal or chemical denaturation with the behavior obtained from potentiometric $H^+$ titration curves. For chymotrypsin (*20*) and ribonuclease A (*21*), the pH dependence of stability obtained by the two different thermodynamic approaches was virtually identical. In the case of SNase, a striking discrepancy was found between the pH dependence of stability obtained by these two independent methods. This finding offers considerable new insight about the structural and thermodynamic character of the denatured ensemble of SNase, and it has important implications about the structural meaning of stability measured by chemical or thermal denaturation for this protein and its mutants.

## EXPERIMENTAL PROCEDURES

SNase was expressed and purified following the procedure described previously by Shortle and Meeker (*22*). The purity of the protein was established to be >98% by SDS−PAGE. Protein concentrations were determined at 280 nm using an optical density of 0.93. All measurements were performed at 20.0 ± 0.1 °C.

*Acid/Base Titration Monitored by Fluorescence and CD.* Acid unfolding was monitored by intrinsic fluorescence of Trp-140 ($\lambda_{ex}$ = 296 nm, $\lambda_{em}$ = 326 nm). All measurements were performed with an AVIV automated titration spectrofluorometer (model ATF-105) equipped with Hamilton MicroLab 531C automated burets. The fluorescence measured at every point represents a signal averaged over 10 s. Samples consisted of 2.7 mL of approximately 50 $\mu$g/mL SNase in 10 mM HEPES + 100 mM NaCl. The titrant was 0.1 N HCl or NaOH. One minute was allowed for equilibration after each dose of titrant was delivered and before

fluorescence was measured. pH was measured with a combination electrode from Orion (model 8102) and an Orion benchtop pH/ISE meter (model 720 A). CD signals were measured at 215, 222, and 275 nm with an Aviv circular dichroism spectrometer (model 62A DS). Signals at 215 and 222 nm were measured with 2.0 mL of approximately 50 $\mu$g/mL SNase in 10 mM HEPES and 100 mM NaCl. At 275 nm, the experiments were performed with 2.0 mL of 1 mg/mL SNase.

The acid/base titration of fluorescence was analyzed assuming two-state behavior (*23*). Fluorescence intensity as a function of pH, $F_{pH}$, can be represented as $F_{pH} = (f_n + f_u K_{app})/(1 + K_{app})$, where $f_n$ and $f_u$ represent the equations for the native and denatured baselines, respectively, and $K_{app} = [U_A]/[N]$ (*20*). According to the theory of linked functions, the number of $H^+$ bound or released concomitant with the proton-linked conformation transition ($\Delta\nu_{H^+}$) is equal to $\partial \ln K_{app}/2.3\ \partial pH$. Therefore,

$$F_{pH} = [f_n + f_u \exp(\beta + 2.3\Delta\nu_{H^+}\ pH)]/[1 + \exp(\beta + 2.3\Delta\nu_{H^+}\ pH)] \quad (1)$$

where $K_{app} = \exp(\beta + 2.3\Delta\nu_{H^+}\ pH)$, and $\beta$ is an integration constant. $\Delta\nu_{H^+}$ was obtained by fitting eq 1 to the data with the NONLIN program for nonlinear least-squares fitting (*24*). $pH_{mid}$, the midpoint along the acid unfolding transition, was calculated analytically from the inflection point in the first derivative of $F_{pH}$ with respect to pH.

*Urea and GdnHCl Denaturation.* $\Delta G°$ at different pH values were measured by automated GdnHCl and urea denaturation monitored by fluorescence ($\lambda_{ex} = 296$ nm, $\lambda_{em} = 326$ nm) as described previously (*22*, *25*). Phosphate buffer, which has been used in most previous studies of denaturational energetics of SNase, was avoided. The pH of phosphate buffer is GdnHCl-sensitive in the concentrations of GdnHCl needed to denature SNase. The interactions between phosphate groups are screened effectively by the ionic strength, depressing the $pK_a$ of the moiety responsible for buffering near neutral pH. Instead, measurements were performed with protein concentrations of approximately 50 $\mu$g/mL in 25 mM HEPES and 100 mM NaCl. All measurements were performed with the Aviv automated titration fluorometer. Titrant consisted of 8.0 M urea or 6.0 M GdnHCl (ultrapure grade, Gibco) plus buffer and salt. Final GdnHCl or urea concentrations were measured with a Milton Roy Abbe-3L refractometer. Five minutes were allowed for equilibration between titration points. The data were analyzed assuming two-state behavior following the method of Bolen and Santoro (*20*). The stability of SNase extrapolated to zero denaturant concentration ($\Delta G°$) and the $m$ values ($d\Delta G°/d[\text{denaturant}]$) were obtained by nonlinear least-squares fitting of eq 2. $f_n$ and $f_u$ represent line equations for the native

$$F_{denat} = \frac{f_n + f_u \exp[-(\Delta G° + m_{\Delta G}[denat])/RT]}{1 + \exp[-(\Delta G° + m_{\Delta G}[denat])/RT]} \quad (2)$$

and denatured baselines, respectively, and $F_{denat} = (f_n + f_u K_{app})/(1 + K_{app})$, and $K_{app} = [D]/[N]$.

*Temperature Denaturation.* $\Delta G°$ values were also determined by thermal denaturation monitored by fluorescence ($\lambda_{ex} = 296$ nm, $\lambda_{em} = 326$ nm) with the AVIV automated titration fluorometer. Temperature control was provided by a Peltier thermoelectric system. One-minute equilibration was allowed between measurements. Samples consisted of 2.0 mL of protein at a concentration of approximately 50 $\mu$g/mL in 5 mM $KPO_4$, 5 mM potassium acetate, and salt. Analysis of the temperature dependence of fluorescence ($F_T$) was also performed assuming two-state behavior. Equation 3 was fitted to the experimental data with nonlinear least squares:

$$F_T = (f_n + f_u \exp[-(\Delta G°(T)/RT)])/(1 + \exp[-\Delta G°(T)/RT]) \quad (3)$$

where

$$\Delta G°(T) = \Delta H(T_m)[1 - T/T_m] - \Delta C_p[(T_m - T) + T \ln(T/T_m)] \quad (4)$$

In eq 4, $T_m$ is the midpoint temperature, $\Delta C_p$ is the change in heat capacity during thermal denaturation, and $\Delta H$ ($T_m$) is the enthalpy change at $T_m$. A $\Delta C_p$ of 2.32 kcal (mol K)$^{-1}$ was used in the initial fit (*18*).

$T_m$ values were resolved with very high precision (± 0.5 °C) by fitting with eq 3. The uncertainties in $\Delta H(T_m)$, however, were large, as high as 10%. To improve the accuracy and precision with which $\Delta G$(20 °C) was determined, $\Delta C_p$ was also calculated from the slope of the line defined by $\Delta H(T_m)$ and $T_m$ values obtained from experiments at different pH values (*5*). $\Delta C_p$ thus determined and $T_m$ were used to estimate $\Delta H(T_m)$ from the line fit, and values of $\Delta C_p$, $T_m$, and $\Delta H(T_m)$ were in turn used in eq 4 to calculate $\Delta G$(20 °C). The $\Delta C_p$ obtained from the slope of $\Delta H(T_m)$ vs $T_m$ was 1.69 kcal (mol K)$^{-1}$, comparable to the value of 1.8 reported earlier by Shortle, Meeker, and Freire (*26*). When the $\Delta H(T_m)$ vs $T_m$ curve was fitted with two straight lines instead of one, the apparent $\Delta C_p$ obtained by the line fitted to the points below pH 4.5 is lower than the $\Delta C_p$ above pH 4.5 and in exact agreement with the $\Delta C_p$ obtained by DSC in this pH range (*27*, *28*).

*Potentiometric Measurement of $H^+$ Binding Curves.* The potentiometric method for measurement of continuous $H^+$ binding curves has been described elsewhere (*20*, *25*). Measurements under native (100 mM KCl) or hyperstabilizing (100 mM KCl + 1.5 M sucrose) conditions were done with a Radiometer PHM 95 pH/ion meter equipped with a Radiometer glass electrode (model PHG201) and a Radiometer calomel reference electrode (model K4040). Measurements in the presence of GdnHCl were performed with a calomel combination electrode (model GK2701). A Radiometer TTA80 titration assembly was used for all measurements.

Titrant dosing was done with a Brinkmann 665 Dosimat (Metrohm, LTD, Switzerland). Titrant consisted of degassed 0.1 N HCl + 100 mM KCl or 0.1 N NaOH + 100 mM KCl (J. T. Baker, 1 N diluted with degassed $H_2O$). The normality of the titrant was determined by the Gran plot analysis method using oven-dried MES buffer. Samples were kept in a $CO_2$-free environment during preparation and during the titration. All samples were prepared with extensively degassed and deionized water. Protein concentrations between 2 and 4 mg/mL were used. No concentration dependence has ever been observed in the $H^+$ titration experiment with SNase in this range of concentration (*25*). After an initial

and extensive dialysis at 4 °C, samples were tabletop centrifuged. They were then dialyzed overnight in a $CO_2$-free atmosphere against 100 mM KCl at 4 °C. Blanks consisted of 3 mL of the dialysis buffer. Multiple titration curves were always measured in each set of conditions, and reversibility was checked routinely. Titration curves were fitted with ninth order polynomials by nonlinear least-squares fitting.

*Direct Measurement of $H^+$ Bound or Released during Structural Transitions.* Batch experiments were performed to measure the number of $H^+$ that were bound or released at a given pH when SNase was diluted to a final concentration of 6 M GdnHCl or 1.5 M sucrose. Samples and titrant were prepared as for continuous $H^+$ titrations. In one set of experiments (water blanks), titrant (HCl + KCl) was added to 4.5 mL of degassed 6.67 M GdnHCl + 100 mM KCl until the pH matched that of the water used in the dialysis. A total of 0.5 mL of the dialysis water was then added to obtain 5 mL of a solution of 6 M GdnHCl + 100 mM KCl. Changes in pH were recorded, and the results of several such measurements were averaged. In another set of experiments, titrant was added to 4.5 mL of degassed 6.67 M GdnHCl + 100 mM KCl until the pH matched that of the dialyzed protein solution. A total of 0.5 mL of protein solution was then added to obtain a 5-mL solution of 1 mg/mL SNase in 6 M GdnHCl + 100 mM KCl. Changes in pH upon addition of the protein were noted, and then the sample was back-titrated with 1-$\mu$L doses of titrant to the original pH of the protein solution. The pH was also adjusted for the pH change observed in the water blank during dilution. The moles of $H^+$ bound per moles of protein were calculated from the titrant volume, its normality, and the number of moles of protein. A similar procedure was used to measure the effects of 1.5 M sucrose on the state of protonation of SNase.

## RESULTS

*Acid/Base Titrations Monitored by Fluorescence and by Potentiometry under Native and Unfolding Conditions.* Acid/base titrations monitored by CD at 222 nm and by intrinsic fluorescence are shown in Figure 1, panel A. The acid unfolding profile agrees with the ones published previously (*9*, *29*−*31*). The steep slope of the acid unfolding transition is consistent with a highly cooperative process. The agreement between transitions monitored by fluorescence and by CD suggests that the transition only involves two states. Forward and reverse titrations were superimposable, thus establishing that the reaction monitored was reversible and at equilibrium. The pH at the midpoint of the unfolding transition ($pH_{mid}$) was 3.71 ± 0.02.

Potentiometric $H^+$ titrations measured in 100 mM KCl and in 6 M GdnHCl + 100 mM KCl are also shown in Figure 1, panel A. Forward and reverse potentiometric titrations were superimposable. They show that in the pH range 9 to $pH_{mid}$, $H^+$ were bound preferentially by the state achieved in 6 M GdnHCl (U state) relative to the N state. The distance between the two $H^+$ titration curves was determined explicitly with a series of batch experiments that measured the number of $H^+$ bound by SNase at a fixed pH upon addition of GdnHCl to a final concentration of 6 M (Figure 1, panel B). The difference $H^+$ binding curve ($\Delta\nu_{H^+}$) in Figure 1, panel B, represents the net number of $H^+$ bound preferentially

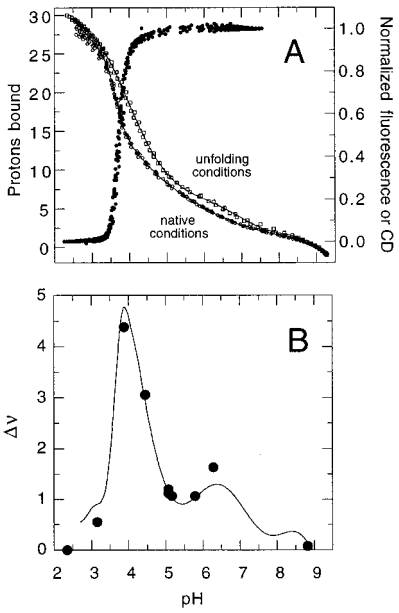


FIGURE 1: (A) $H^+$ titration curves measured potentiometrically (left axis) in 100 mM KCl (open circles) and in 6 M GdnHCl + 100 mM KCl (open squares). Data from multiple experiments, including forward and reverse titrations, are included in each curve. The solid lines through the data represent fits with ninth order polynomials. The distance between the two $H^+$ binding curves along the ordinate was established with the data shown in panel B. Acid/base titration in 100 mM KCl monitored by fluorescence and by $CD_{222\ nm}$ (solid circles) are also shown (right axis). (B) Difference in $H^+$ bound in 6.0 M GdnHCl and in 100 mM KCl, measured as difference of the continuous titration curves in panel A (solid line) and with batch experiments (dots). The diameter of the dots is larger than the experimental uncertainties.

by the U state relative to the N state. This $\Delta\nu_{H^+}$ curve reflects the overall higher $H^+$ affinity of the U state relative to the N state. The agreement between the $\Delta\nu_{H^+}$ values measured independently by continuous and by batch potentiometric experiments was excellent.

The shape of the $\Delta\nu_{H^+}$ binding curve can be interpreted as follows. The hump centered near pH 6.5 is indicative of net depressed p$K_a$ values of histidines in the N state. The increase in the number of $H^+$ bound preferentially by the U state between pH 5 and pH 4 reflects depressed p$K_a$ values of acidic residues in the N state. The maximum at pH 3.95, where 4.8 $H^+$ were bound preferentially by the U state, coincided with the pH of onset of acid denaturation monitored by fluorescence and CD (Figure 1, panel A). In 100 mM KCl, SNase begins to unfold at pH 4, thus the sign of the slope of the $\Delta\nu_{H^+}$ curve changed concomitant with an increase in the population of the acid unfolded state ($U_A$). The quality of the data measured by the continuous $H^+$ titration method declined below pH 3, although the difference curves are still reliable, as shown by the agreement between continuous and batch measurements. According to the batch experiments in Figure 1, panel B, 0.5 $H^+$ were bound upon addition of GdnHCl to a final concentration of 6.0 M at pH 3.2, and 0 $H^+$ were bound at pH 2.4.

The analysis of the pH titration monitored by fluorescence in Figure 1, panel A, with Wyman's linkage relationships showed that 4.18 ± 0.1 $H^+$ were bound during the acid-induced transition between N and $U_A$ states. This is in very close agreement with the number of $H^+$ shown to be bound preferentially to the U state by the potentiometric methods

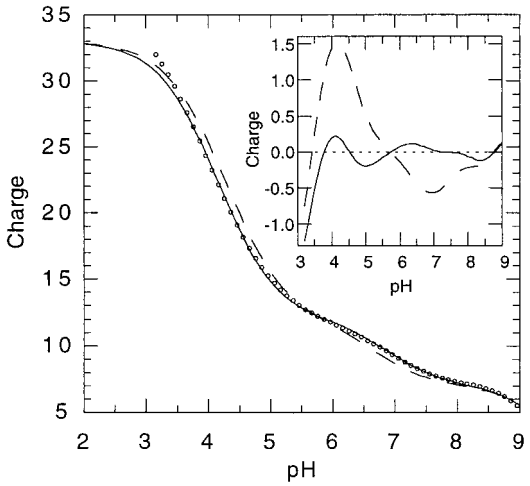


FIGURE 2: Experimental (open circles) $H^+$ titration of SNase in 6 M GdnHCl and curves simulated with p$K_a$ values for Asp, Glu, and His of 4.0, 4.5, and 6.6, respectively (dashed) and with p$K_a$ values of 3.88, 4.38, and 6.83 (solid). Insert: difference between experimental and simulated curves.

(Figure 1, panel B). This agreement suggests that the unfolded states achieved in acid and in 6 M GdnHCl are nearly equivalent from the standpoint of their $H^+$ binding affinity. This was corroborated by the data in Figure 1, panel B, which show that at pH < 3 the $H^+$ binding properties of the U and $U_A$ are equivalent.

*p$K_a$ Values in the GdnHCl-Unfolded State.* p$K_a$ values of ionizable groups are sensitive to their local environments. In the case of highly charged proteins such as SNase, p$K_a$ values can also be influenced significantly by the net charge of the protein, and they can be highly sensitive to the ionic strength of the solution. The p$K_a$ values of ionizable groups of folded proteins are usually spread over a broad range, reflecting primarily the heterogeneity of their microenvironments. Ionizable groups are therefore effective reporters of the presence of structure and compactness.

Tanford demonstrated that the spread in p$K_a$ values is lost in the unfolded state of proteins that denature into near-random coils in high concentrations of GdnHCl (*32*−*34*). In the unfolded states of these proteins, the p$K_a$ values of all ionizable residues converge at the values measured for model compounds in GdnHCl. This convergence is associated primarily with the substantial loss of structure, although it also reflects the screening of interactions between charged groups by the high ionic strength of GdnHCl. High ionic strength comparable to that of denaturing concentrations of GdnHCl do not force convergence of p$K_a$ values to a common value in the N state because some of the factors that determine p$K_a$ values are not salt-sensitive (*1*, *14*, *35*).

Proton titration curves of non-native states of proteins can be used effectively to detect the presence of residual structure. To determine if residual structure was present in GdnHCl-unfolded SNase, the $H^+$ titration curve measured in 6 M GdnHCl was simulated by treating the 61 ionizable sites (8 Asp, 12 Glu, 23 Lys, 5 Arg, 4 His, 7 Tyr, and N and C termini) with the set of model compound p$K_a$ values commonly used in structure-based p$K_a$ calculations. These are 3.5 for C terminus, 4.0 for Asp, 4.5 for Glu, 6.6 for His, 7.4 for N terminus, 10 for Tyr, 10.4 for Lys, and 12.0 for Arg (*4*). The agreement between the observed and predicted behavior (Figure 2) was extremely good, suggesting that in 6 M GdnHCl the p$K_a$ values converged at the values of model compounds. The small systematic deviation (Figure 2, insert) suggests that in 6 M GdnHCl there are slight increases in the p$K_a$ values of basic residues and slight decreases in the p$K_a$ values of acidic residues, relative to p$K_a$ values of model compounds in water.

Also shown in Figure 2 is one of the best fits to the $H^+$ titration curve in 6 M GdnHCl, obtained by assuming that all residues of a given type titrate with identical p$K_a$ values. This assumption was necessary because it was impossible to find a unique combination of 61 p$K_a$ values with which to fit the $H^+$ titration curve of the U state. The best fits were those in which the p$K_a$ values of Asp, Glu, and His residues were 3.88, 4.38, and 6.83, respectively. These values are almost identical to the values obtained by Tanford and co-workers from analysis of $H^+$ titration curves of other proteins in high concentrations of GdnHCl (*32*, *33*). The similarity in the ionization behavior of Asp, Glu, and His residues in water and in 6 M GdnHCl suggests that the hydration of the charged species in the ionization equilibria is not disrupted significantly in 6 M GdnHCl, as noted earlier by Tanford (*32*−*34*). The differences between the p$K_a$ values of model compounds in water and those extracted from the $H^+$ titration curve of SNase in 6 M GdnHCl (4.00 vs 3.88 for Asp, 4.50 vs 4.38 for Glu, and 6.83 vs 6.60 for His) were consistent with the effects of increasing salt concentrations on ionization equilibria (*35*). Under conditions of high ionic strength the charged form of the ionizable groups is selected preferentially over the neutral form, resulting in the increase or decrease of p$K_a$ values of basic or acidic groups, respectively.

The data in Figure 2 demonstrate that in 6.0 M GdnHCl the ionizable groups of SNase titrated with p$K_a$ values nearly identical to those of model compounds. This behavior is consistent with that of an extended and presumably unstructured, highly solvated, highly screened form of the protein in which the ionizable groups are all isolated from each other, fully hydrated, and not under the influence of other charged or polar groups. Under these conditions, all electrostatic influences on p$K_a$ values were annulled. The state achieved in 6.0 M GdnHCl is termed the U state throughout this paper. The point of this nomenclature is to distinguish the U state from the D state that is populated under less drastic conditions during equilibrium unfolding experiments and to emphasize the absence of electrostatic effects in this unfolded state, as reflected in average p$K_a$ values.

*Acid/Base Titration Monitored by Fluorescence and Potentiometry under Hyperstabilizing Conditions.* For reasons discussed ahead, it was necessary to measure $H^+$ binding to the N state at pH < $pH_{mid}$. Toward this end, the pH range in which the N state is populated was expanded artificially by addition of sucrose to a final concentration of 1.5 M. Sucrose was selected from among the osmolytes known to enhance the stability of globular proteins because it is not charged and because it stabilizes SNase at molalities low enough to avoid problems related to the high viscosity of osmolytes in the automated denaturation experiments. Hydrolysis of sucrose is negligible in the pH range where it was used.

The acid/base titration of fluorescence in Figure 3, panel A, shows that the $pH_{mid}$ of acid denaturation was shifted from 3.71 to 3.11 ± 0.2 as a result of the stabilization of the N state by 1.5 M sucrose. At pH > 4, the $H^+$ titration curves measured with and without sucrose were nearly superim-

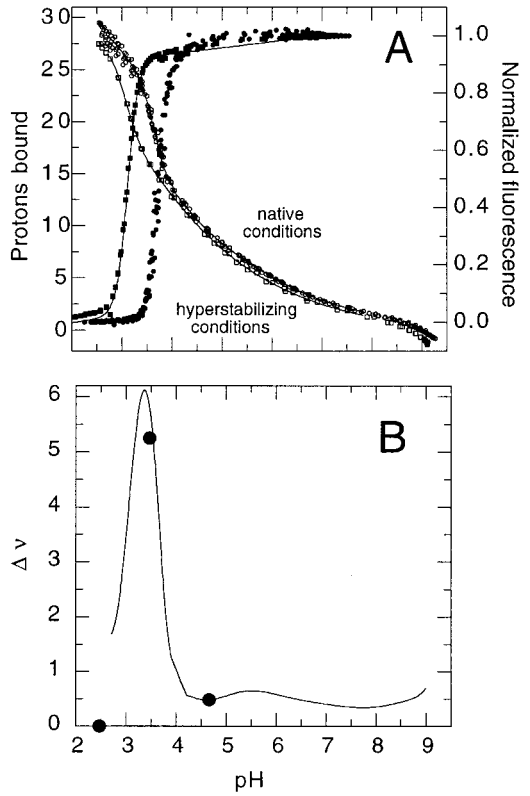


FIGURE 3: (A) $H^+$ titration curves measured potentiometrically (left axis) in 100 mM KCl (open circles) and in 1.5 M sucrose plus 100 mM KCl (open squares). Solid lines through these data represent fits with ninth order polynomials. The distance between these two curves along the ordinate was determined by the data shown in panel B. Fluorescence-monitored acid/base titration in 1.5 M sucrose plus 100 mM KCl (solid squares) and in 100 mM KCl without sucrose (solid circles) are also shown (right axis). (B) Difference in $H^+$ binding behavior in 100 mM KCl and in 100 mM KCl + 1.5 M sucrose, measured as difference of the continuous titration curves in panel A (solid line) and with batch experiments (dots). The diameter of the dots is larger than the experimental uncertainties.

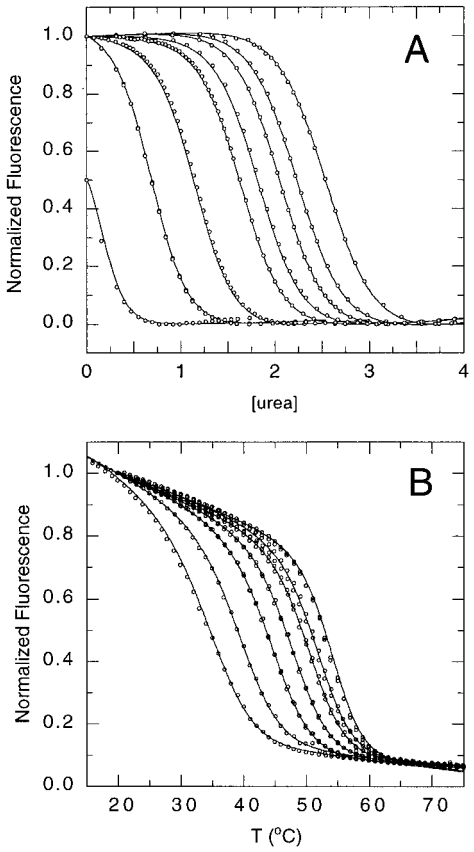


FIGURE 4: (A) Urea denaturation monitored by fluorescence in 100 mM KCl at pH (left to right) 3.69, 4.06, 4.45, 5.01, 5.53, 6.05, 6.54, 7.98. (B) Temperature denaturation in 100 mM KCl monitored by fluorescence at pH (left to right) 4.00, 4.20, 4.50, 4.80, 5.23, 5.53, 7.93. The lines through the data in both panels represent the fits as described in Experimental Procedures.

posable. The small differences suggest that the p$K_a$ values of histidines are depressed slightly in the presence of sucrose. 1.5 M sucrose has no direct effect on the p$K_a$ values of acidic residues. This was confirmed by showing that there are no differences in the p$K_a$ values of glycine, acetic, and oxalic acids measured potentiometrically in the presence and in the absence of 1.5 M sucrose. In 100 mM KCl, the p$K_a$ values of acetic acid, oxalic acid, and glycine were 4.64, 3.79, and 2.45, respectively, while in 1.5 M sucrose plus 100 mM KCl, they were 4.59, 3.73, and 2.39.

The distance between the two $H^+$ binding curves in Figure 3, panel A, was established by measuring the number of $H^+$ bound or released upon addition of sucrose to a final concentration of 1.5 M at a fixed pH (Figure 3, panel B). The continuous $\Delta\nu_{H^+}$ curve calculated by subtracting the $H^+$ titration curves measured with and without sucrose is shown in Figure 3, panel B. Between pH 3.4 and 4.1, the $\Delta\nu_{H^+}$ curve in Figure 3, panel B, mirrors the acid/base titration monitored by fluorescence in 100 mM KCl shown in Figure 1, panel A, because they both reflect the highly cooperative transition between N and $U_A$ states.

*pH Dependence of Stability Measured by Temperature and Chemical Denaturation.* SNase was selected for these studies deliberately because it can be coaxed into denatured states easily. It offers ample opportunities to characterize thermodynamic properties of structured, compact denatured states. It was also selected because it is devoid of disulfide bridges and other structural features that could bias the structure of the denatured state or complicate denaturation in other ways. Its chemical (*16*), acid (*9*, *27*), and temperature (*15*, *18*, *27*, *28*, *36*) denaturation are known to be fully reversible, and at least under conditions of low salt, SNase remains monomeric and highly soluble over the wide range of pH that was studied (*37*).

Urea and temperature denaturation curves measured in 100 mM NaCl over a range of pH values are shown in Figure 4. All the transition curves exhibited the sigmoidal shape expected of an apparent two-state process. The denaturation at each pH was analyzed by the linear extrapolation method assuming two-state behavior, and the fits showed no evidence of the presence of a stable intermediate. The pH dependence of stability measured by urea, GdnHCl and temperature denaturation is shown in Figure 5. The $\Delta G^o_{Gdn}$ values are comparable to values reported previously by other investigators (*17*, *36*). Overall, the pH dependence of $\Delta G^o_{urea}$ and $\Delta G^o_T$ was very similar. The values of $\Delta G^o_{urea}$ and $\Delta G^o_T$ above pH 7 were not identical; they were within error only because of the stringent treatment of errors in the estimation of $\Delta G^o_T$ and because the large error bars in $\Delta G^o_{urea}$ reflect the average of values from several experiments. However, the overall similarity in the pH dependence of $\Delta G^o_{urea}$ and $\Delta G^o_T$

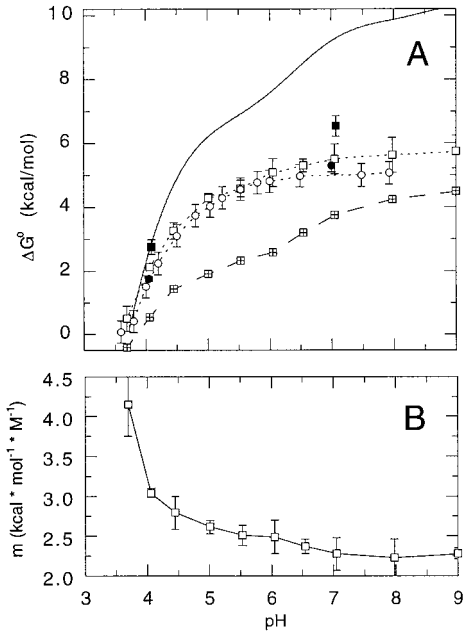


FIGURE 5: (A) pH dependence of the stability of SNase at 20 °C in 100 mM NaCl obtained by fluorescence-monitored denaturation with urea (open squares), GdnHCl (solid circles), temperature (open circles), and by numerical integration of the $H^+$ binding curves in Figure 1 (solid line). Also shown at pH 4 and pH 7 are $\Delta G^o_{urea}$ in 1.0 M NaCl (solid squares). The large uncertainties in $\Delta G^o_{urea}$ obtained by urea denaturation at pH ≥ 6 reflect errors from averages of multiple experiments rather than errors of the fits of single experiments. The uncertainty in the $\Delta G^o_{pH}$ of any single experiment is usually of the order of ± 0.1 kcal/mol. The large error bars of approximately 0.35 kcal/mol in $\Delta G^o_T$ reflect the uncertainties in the $\Delta H(T_m)$, $\Delta C_p$, enhanced by the extrapolation to 20 °C. Hatched squares represent the difference between stability measured by urea denaturation and by numerical integration of $H^+$ binding curves. (B) pH dependence of the *m* values of urea denaturation.

suggests that the $H^+$ binding properties of temperature and urea-denatured ensembles are similar.

The pH at which $\Delta G^o_{urea}$, $\Delta G^o_{Gdn}$, and $\Delta G^o_T$ are zero coincides with the $pH_{mid}$ measured by acid/base titration of fluorescence and CD (Figure 1, panel A). According to $\Delta G^o_T$ and $\Delta G^o_{urea}$ the stability of SNase is not highly pH-sensitive in the range 9 to 5. In this range, stability decreases by 1.7 kcal/mol. At pH values <5, however, the loss of stability is more pronounced, reflecting the average higher $H^+$ binding affinity of acidic residues in the D state relative to the N state.

Also shown in Figure 5 are $\Delta G^o_{urea}$ values that were measured in 1.0 M NaCl at pH 4 and pH 7 to assess the influence of the ionic strength of GdnHCl solutions. Note that at pH 4 and pH 7, the stability of SNase measured by $\Delta G^o_{urea}$ and $\Delta G^o_{Gdn}$ in 100 mM NaCl are almost identical. In fact, at pH 7 in 100 mM NaCl, $\Delta G^o_{urea}$ and $\Delta G^o_{Gdn}$ are more similar to each other than they are similar to $\Delta G^o_T$. However, the stability reported by $\Delta G^o_{urea}$ in 1.0 M NaCl and by $\Delta G^o_{Gdn}$ are different, suggesting that denaturational $\Delta G°$ values are not just a function of the protein but also of ionic strength and of the chemical denaturant used to measure them. According to $\Delta G^o_{urea}$, the stability of SNase in 1 M NaCl is 1 kcal/mol greater than the stability in 100 mM NaCl. This suggests that both N and D states are highly sensitive to the ionic strength and that the thermodynamic character of the denatured ensembles achieved in GdnHCl and in urea at low ionic strength are different. $\Delta G^o_{Gdn}$ were not studied over the entire pH range to avoid complications arising from the sensitivity of both N and D states to the ionic strength.

*pH Dependence of Stability Measured from Potentiometric $H^+$ Titration Curves.* Also shown in Figure 5 is the pH dependence of stability calculated by numerical integration of potentiometric $H^+$ titration curves ($\nu_{H^+}$) measured under native (100 mM KCl) and unfolding (6.0 M GdnHCl) conditions. The integration was performed with eq 5. The

$$\Delta G^\circ_{\Delta\nu} = -2.303RT \int_{pH_1}^{pH_2} (\nu^U_{H^+} - \nu^N_{H^+})\, dpH \qquad (5)$$

term inside this integral in eq 5 corresponds to the $\Delta\nu_{H^+}$ curve shown in Figure 1, panel B.

The distance between the stability curve calculated with eq 5 and the one determined by fluorescence-monitored denaturation experiments was adjusted by fixing $\Delta G^o_{\Delta\nu} = 0$ at $pH_{mid}$, where, by definition, the population of N and $U_A$ states are equal. This manipulation was required to enable the comparison of $\Delta G^o_{\Delta\nu}$ with $\Delta G^o_T$, with $\Delta G^o_{urea}$, and with $\Delta G^o_{Gdn}$ in absolute terms. The implicit assumptions when performing this adjustment are that the $H^+$ titration properties of the U and $U_A$ states are identical and that acid unfolding is a two-state process. The validity of the approximation of the treatment of the acid unfolding transition with a two-state mechanism was supported by the steepness of the acid denaturational transitions and by the agreement between the acid/base titration monitored by fluorescence and CD (Figure 1, panel A). The assumption that the $H^+$ binding properties of U and $U_A$ states are nearly identical at low pH was supported by the two $H^+$ titration curves in Figure 1, panel A, which converge as the population of N is replaced by $U_A$ in the titration curves measured in 100 mM KCl. Further evidence was provided by the batch experiments showing that at pH < 3 nearly identical numbers of $H^+$ are bound by $U_A$ and U states. A similar conclusion would have been reached through the observation that the $\Delta\nu_{H^+}$ curve in Figure 1, panel B (U minus N) and the curve in Figure 3, panel B ($U_A$ minus N) intersect at $pH_{mid}$. This would not occur if the $H^+$ binding properties of U and $U_A$ were substantially different. Whatever differences might exist between $H^+$ binding properties of $U_A$ and U they represent a small amount of the total area under the $H^+$ binding curve used to estimate $\Delta G^o_{\Delta\nu}$. Note that the significant discrepancy between $\Delta G^o_T$, $\Delta G^o_{urea}$, and $\Delta G^o_{\Delta\nu}$ is independent of any errors introduced by assuming that U and $U_A$ are identical from the perspective of their $H^+$ binding properties. The differences between the stability curves determined by different methods are independent of how the stability curve described by $\Delta G^o_{\Delta\nu}$ is fixed relative to the other stability curves. If the $\Delta G^o_{\Delta\nu}$ curve had been frame-shifted arbitrarily along the ordinate to match $\Delta G^o_{urea}$ at any pH, the difference between stabilities measured by two different methods would still be largest in the pH range 4.5 to 9. In other words, $\Delta\Delta G^o_{\Delta\nu}$ between any two pH values above pH 4, where the population of the $U_A$ state is negligible, is considerably larger than the $\Delta\Delta G^o_T$ or $\Delta\Delta G^o_{urea}$ over the same range of pH.

In the region between $pH_{mid}$ and the pH where the acid denaturational transition begins (pH 4.1), the $H^+$ titration in

100 mM KCl reflects $H^+$ binding contributions not only by the N state but also by the $U_A$ state. To establish the distance between the two stability curves in Figure 5 by fixing $\Delta G^o_{\Delta\nu} = 0$ at $pH_{mid}$, it was necessary to account for the free energy of $H^+$ binding to the N state that would accrue between $pH_{mid}$ and pH 4.1. The $H^+$ titration curve of sucrose-stabilized SNase was used toward this end. The free energy between $pH_{mid}$ and pH 4.1 was estimated by numerical integration of the $\Delta\nu_{H^+}$ curve obtained by summing the curves in Figure 1, panel B, and Figure 3, panel B, between pH 3.71 to pH 4.10.

The discrepancy between the pH dependence of stability determined by denaturation and by numerical integration of $H^+$ titration curves is striking. A curve is included in Figure 5 to show the pH dependence of the difference between the two stability curves. The destabilization of N relative to U between pH 9 and pH 4 reported by $\Delta G^o_{\Delta\nu}$ was nearly 4 kcal/mol greater than the destabilization of N relative to D reported by $\Delta G^o_T$ and $\Delta G^o_{urea}$ in the same pH range. At pH 7, the stability of SNase according to $\Delta G^o_{\Delta\nu}$ was approximately 3.7 kcal/mol greater than the previously reported values near 5.5 kcal/mol measured by temperature or chemical denaturation (*16*, *36*). The agreement between $\Delta G^o_{urea}$, $\Delta G^o_{Gdn}$, and $\Delta G^o_T$ suggests that this discrepancy did not simply arise from differences in the denatured states achieved in water and in the presence of chemical denaturants. It is important to note that the stability measured by analysis of the hydrogen exchange behavior of the slowest exchanging backbone amides (*38*) is more consistent with the stability reported by $\Delta G^o_{\Delta\nu}$ than with the one described by $\Delta G^o_T$ or $\Delta G^o_{urea}$.

## DISCUSSION

Structure-based calculations of the pH dependence of stability of proteins with methods based on continuum electrostatics are usually performed under the assumption that the p$K_a$ values of ionizable residues in the D states of proteins are those of model compounds in water (refs *1*, *4*, *40*, *41*, and refs therein). This assumption was originally supported by the pioneering studies by Tanford and co-workers (*32*−*34*), who demonstrated that the $H^+$ titration of some proteins in 6 M GdnHCl followed the behavior predicted from the p$K_a$ values of model compounds. In general, structure-based estimates of proton-linked stability of proteins capture the overall trends correctly (*40*, *41*). However, with a few exceptions, quantitative agreement between calculated and observed behavior is still rare. Because the quantitative estimation of electrostatic free energies and p$K_a$ values from structure with computational methods based on continuum electrostatics remains a daunting task, the lack of quantitative agreement could be easily dismissed as the result of methodological problems inherent to the structure-based calculations. However, recent studies suggest that some of the problems arise from the assumption that the p$K_a$ values of ionizable residues in the D states of proteins are those of model compounds in water (*5*−*7*, *13*, *14*). This assumption is not valid for many proteins because electrostatic effects in non-native states can be significant, presumably because they are structured and compact.

In this study of the contributions by electrostatic interactions to the stability of SNase it would have been inappropriate to make assumptions about the $H^+$ titration properties of the D state because it is known to be structured and compact (*15*−*17*, *19*). In fact, our original attempts to interpret the pH dependence of stability of SNase structurally, with structure-based p$K_a$ calculations, failed dramatically. The data in this study demonstrate that those calculations failed primarily because the underlying assumption that ionizable groups in the D state titrate with the p$K_a$ values of model compounds in water (or in GdnHCl) is not valid for SNase. The $H^+$ binding properties of the N and U states measured potentiometrically suggest that the $H^+$ binding properties of the D state are intermediate between those of N and U states. Evidently there are strong, presumably long-range electrostatic interactions in the D state, and these are reflected in perturbed p$K_a$ values.

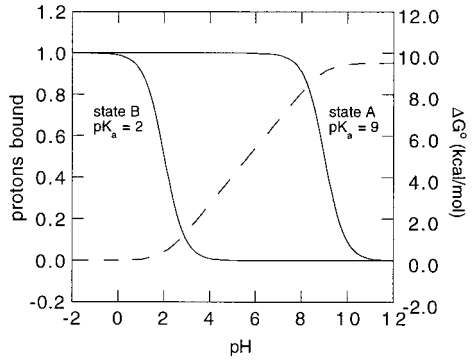


FIGURE 6: Simulation of the $H^+$ titration curves (solid lines) of an ionizable group that titrates with p$K_a$ of 2 in state A and with p$K_a$ of 9 in state B, as labeled, and pH dependence of the free energy difference (dashed line) between these two states calculated by numerical integration of the area between the two titration curves.

*Meaning of $\Delta G^o$ Obtained by Integration of $H^+$ Titration Curves.* The numerical integration of $H^+$ titration curves to obtain $\Delta G^o_{\Delta\nu}$ is not a transformation familiar to many. The data in Figure 6 were simulated to illustrate how the pH dependence of the free energy difference between two states in equilibrium can be obtained by analysis of the $H^+$ titration properties of the two end states. In this example, the pH dependence of the equilibrium between states A and B is determined by the difference in the p$K_a$ value of a single group that titrates with p$K_a$ of 2 in state A and with p$K_a$ of 9 in state B. The $\Delta G^o_{\Delta\nu}$ represented by the difference in p$K_a$ values is maximal under conditions of pH where the ionizable site in both states A and B is fully deprotonated or protonated. For p$K_a$ values of 2 and 9 this $\Delta G^o_{\Delta\nu} = \Delta pK_a \times 1.34 = 9.52$ kcal/mol at 20 °C.

The pH dependence of the free energy difference between states A and B is proportional to the area between the titration curves. It can be calculated (in kcal/mol) as a function of pH by numerical integration of this area with eq 5. The total area between the two titration curves in Figure 6 represents a free energy equal to $\Delta pK_a \times 1.34$ kcal/mol (20 °C). The slope of the $\Delta G^o_{\Delta\nu}$ vs pH curve in the linear region, where one site is fully protonated and the other one remains fully unprotonated, is 1.34 kcal/mol (the difference in chemical potential for a log unit change in $H^+$ concentration). The integration of difference titration curves yields relative free energy differences between two states at two pH values.

This example illustrates how numerical integration of $H^+$ titration curves can be used to calculate the pH dependence of an equilibrium process. In this example, the pH-dependent

Scheme 1

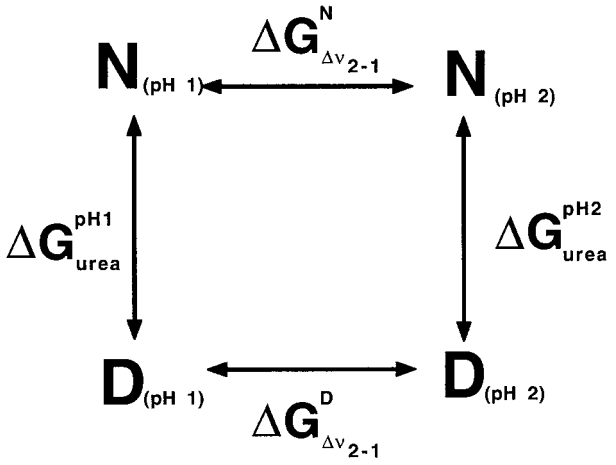


behavior arises from the difference in the ionization properties of a single group. The calculation of $\Delta G^{o}_{\Delta\nu}$ in the case of multisite $H^+$ binding systems is entirely analogous; the approach is valid regardless of the number of ionizable sites that poise the equilibrium for regulation by pH. The $\Delta G^{o}_{\Delta\nu}$ values obtained by numerical integration are completely model-independent, and in general they are more precise than the ones determined by denaturation (*20*, *21*, *25*). This thermodynamic formalism applies to all ligand linked conformation equilibria.

These thermodynamic relationships have two implications in the case of $H^+$ binding reactions. First, when the average $H^+$ affinity is higher in the D state (i.e., higher p$K_a$ values) than in the N state, the stability of the protein will decrease as the concentration of $H^+$ increases—the state with the high affinity for $H^+$ is selectively stabilized as the $H^+$ concentration increases. Second, as p$K_a$ values reflect the effects of the macromolecular milieu on the energy difference between the charged and the neutral forms of the ionizable group, the energies that are calculated by numerical integration of $H^+$ binding curves reflect electrostatic contributions to stability.

*Discrepancy in the pH Dependence of Stability Measured by Different Thermodynamic Methods.* The $\Delta G^{o}_{\Delta\nu}$ obtained by integration of $H^+$ titration curves and the $\Delta G°$ values obtained from equilibrium denaturation experiments are related formally by the thermodynamic cycle in Scheme 1. In this cycle, the reactions along the horizontal branches represent $H^+$ titration under native conditions (100 mM KCl) or at fixed concentrations of GdnHCl higher than those needed to denature SNase. The reactions along the vertical branches represent urea (or heat) induced denaturation at fixed pH values.

Bolen and co-workers used this thermodynamic cycle previously to establish the validity of $\Delta G°$ measured by chemical denaturation for several proteins (*20*, *21*). They demonstrated that $\Delta G^o$ behaved as a function of state by showing that the branches of the cycle were additive (i.e., the sum of the energies in the four branches must equal zero if $\Delta G°$ values are valid thermodynamic functions). This requires that at least three conditions be met: (i) the denaturational transitions along the vertical axes must follow a fixed two-state mechanism and the linear extrapolation method used to extract $\Delta G°$ from equilibrium denaturational transitions must be valid, (ii) the D state populated in the optically monitored denaturation experiments must be thermodynamically equivalent to the U state that is populated at the high concentration of denaturant used in the potentiometric measurement of $H^+$ titration curves, and (iii) the $\Delta\nu_{H^+}$ in the reactions along the vertical axes must occur in the denaturational transition proper and not in the pre- or post-transition zones.

According to the thermodynamic cycle in Scheme 1:

$$\Delta G^{\circ}_{pH_2\rightarrow pH_1} = \Delta G^{N}_{\Delta\nu 2\rightarrow 1} - \Delta G^{D}_{\Delta\nu 2\rightarrow 1} = \Delta G^{\circ}_{urea}(pH_2) - \Delta G^{\circ}_{urea}(pH_1) \quad (6)$$

These equalities were satisfied by the proteins that Bolen and co-workers studied previously with this approach (*20*, *21*), but they are not satisfied by SNase. The data in Figure 5 show that the pH dependence of $\Delta G^{o}_{\Delta\nu}$ measured from $H^+$ titrations of SNase in 100 mM KCl and in 6 M GdnHCl is not equivalent to the pH dependence of denaturational free energies measured by chemical ($\Delta G^{o}_{urea}$) or temperature ($\Delta G^{o}_{T}$) denaturation. This does not necessarily mean that any of the measured $\Delta G°$ values are not valid functions of state. If the $\Delta G°$ values measured by the two different equilibrium thermodynamic methods are meaningful, then the apparent violation of the thermodynamic cycle in Scheme 1 must signal a violation of one or more of the conditions that are required for the cycle to be valid.

The sources of potential error in $\Delta G^{o}_{urea}$ and $\Delta G^{o}_{T}$ are very different from those in $\Delta G^{o}_{\Delta\nu}$. The accuracy of the potentiometric experiments was assessed carefully. These experiments can be fraught with systematic errors, but these can be detected by repeating experiments multiple times. SNase is extremely well-behaved in the potentiometric experiments; the data sets measured by different operators, with different batches of protein, on different days, are indistinguishable. Precipitation has never been detected in the pH range that was studied. The accuracy of $H^+$ titration curves of SNase is high enough to resolve the titration curve of an individual residue by difference of the titration curves measured for the wild type and for a mutant in which the ionizable group of interest is mutated to a neutral residue (*25*).

Five arguments of internal consistency support the validity of $\Delta G^{o}_{\Delta\nu}$ values in Figure 5. First, it was possible to simulate the measured $H^+$ titration behavior in GdnHCl quantitatively by assuming that the 61 ionizable groups titrate with the p$K_a$ values of model compounds. This would have been impossible if these $H^+$ titration curves were systematically in error or otherwise inaccurate. Second, in the $H^+$ titration curve measured under native conditions the pH where the slope changes markedly because of a change in the population from pure N to mixed N and $U_A$, coincided exactly with the pH where the onset of denaturation occurs in the acid/base titration monitored by fluorescence and by CD at 222 nm (Figure 1). Third, there was excellent agreement in the number of $H^+$ bound preferentially by the unfolded state at $pH_{mid}$ measured directly by potentiometry and indirectly by linkage analysis of the acid/base titration monitored by spectroscopic signals. Fourth, the difference $H^+$ binding curves measured by batch and continuous titration experiments were in excellent agreement (Figure 1, panel B). The fifth and final argument confirming the

accuracy and validity of $\Delta G^{o}_{\Delta\nu}$ is the excellent agreement found between the pH dependence of stability described by $\Delta G^{o}_{\Delta\nu}$ in the pH range from 9 to 5 and the one estimated from the difference between native state histidine p$K_a$ values measured by H NMR spectroscopy (*39*) and the denatured state histidine p$K_a$ of 6.8 obtained from the fit of the U state titration curves in Figure 2. The $\Delta$p$K_a$ of histidines predicts that 3.5 kcal/mol of stability are lost between pH 9 and 5, in agreement with the loss of stability in this range of pH described by $\Delta G^{o}_{\Delta\nu}$.

Assessing the validity and meaning of $\Delta G^{o}_{urea}$ and $\Delta G^{o}_{T}$ is complicated by the multiple layers of approximations needed to obtain these values by analysis of denaturational transitions (*19*, *20*). For example, the analysis of denaturational transitions with models that describe the equilibrium process in terms of fixed number of discrete states is one potential source of error. The denaturational transition of SNase is usually analyzed in terms of a fixed two-state (N $\leftrightarrow$ D) mechanism (*16*, *36*), but Carra and Privalov have argued in favor of the three-state mechanism (N $\leftrightarrow$ I $\leftrightarrow$ D) based on DSC data (*18*, *27*, *28*). There is experimental evidence that the denaturation of some mutants of SNase is best described with a three-state model (*17*). However the denaturation of wild type SNase near neutral pH meets the criteria normally considered sufficient to validate analysis of the denaturational transition in terms of a two-state process: (i) the $\Delta G°$ obtained with different spectroscopic probes (CD and fluorescence) and with different denaturants are equivalent (*36*, *38*), (ii) the shape of the denaturational transitions and the quality of the fits achieved with a two-state model were excellent over a wide range of pH values (Figure 4), (iii) the ratio of calorimetric to van't Hoff enthalpies is close to 1 (*36*), and (iv) size exclusion chromatograms, in which the Stokes radii of the different species populated during denaturation are resolved, show that discrete intermediates are not populated (*17*). In fact, the only type of experimental data that suggest that denaturation of the wild type SNase can proceed through a three-state process consists of thermal denaturation studied calorimetrically at very low pH and in the presence of relatively high concentrations of salt (*18*, *27*, *28*). There is simply no convincing evidence at present to support the notion that wild-type SNase denatures through a three-state mechanism at pH > $pH_{mid}$ and at ionic strengths comparable to those used in the present experiments. It is therefore unlikely that the discrepancies in the pH dependence of stability measured by denaturation and by potentiometry arise from not treating the denaturational transitions in terms of a three-state mechanism.

Another possible source of error in $\Delta G^{o}_{urea}$ and $\Delta G^{o}_{T}$ is the extrapolation needed to obtain $\Delta G°$ under conditions other than those where the denaturation is actually observed. SNase denatures at relatively low temperature or denaturant concentrations, thus the extrapolation to 20 °C or zero denaturant concentration is particularly short. One way to establish the validity of the extrapolation is by comparing $\Delta G^{o}$ values measured by denaturation with different agents. The mode of action of heat, urea, and GdnHCl is quite different, and concordance in the stabilities measured with different denaturants would at least establish that the $\Delta G°$ values are a function of the protein and not of the method used to measure them. At pH 7, $\Delta G^{o}_{urea}$ and $\Delta G^{o}_{Gdn}$ were within confidence limits, although as mentioned already this agreement is not as meaningful as it seems. $\Delta G^{o}_{urea}$ measured in 1 M NaCl is different from $\Delta G^{o}_{Gdn}$, suggesting that the denatured ensembles achieved in urea and in GdnHCl are significantly different. The stability measured by analysis of urea and GdnHCl denaturation by the linear extrapolation method is not a property of the protein alone; it also reflects the nature of the denaturant. Specifically, the high ionic strength of GdnHCl seems to affect the measured energetics significantly.

In contrast, $\Delta G^{o}_{urea}$ and $\Delta G^{o}_{T}$ measured at the same ionic strength are comparable throughout most of the pH range. The heat capacity ($\Delta C_p$) and enthalpy ($\Delta H$) differences between N and D states are the physical parameters needed in eq 4 to extrapolate $\Delta G^{o}_{T}$ measured at $T_m$ to temperatures outside the range where denaturation is actually observed. Uncertainties in $\Delta C_p$ and in $\Delta H$ are amplified by the extrapolation and can result in significant uncertainties in the $\Delta G^{o}_{T}$ calculated at temperatures far from $T_m$. In thermal denaturation observed spectroscopically, the inherent difficulties in the estimation of $\Delta C_p$ can compound the inaccuracies in $\Delta G^{o}_{T}$ at $T < T_m$. This is reflected in the large error bars in $\Delta G^{o}_{T}$ in Figure 5. It is reassuring that the thermodynamic parameters resolved by analysis of thermal denaturation monitored by fluorescence are very similar to the ones obtained previously with optical methods (*26*) and by differential scanning calorimetry (*18*, *27*, *28*). Although the data in Figure 5 suggest that the urea and heat denatured ensembles have similar thermodynamic character, there were measurable differences, especially at pH > 6.5. The hydrodynamic radius of heat-denatured SNase is larger than that of the native state but smaller than the urea-denatured state (*15*). Urea can actually induce further unfolding of temperature denatured SNase (*15*). This is consistent with the $\Delta G^{o}_{T}$ values being slightly lower than $\Delta G^{o}_{urea}$.

Bolen and co-workers demonstrated recently that SNase denatures with a variable two-state mechanism rather than with a fixed two-state mechanism (*17*). The averaged Stokes radius of the molecules in the denatured ensemble of SNase varies during the denaturational transition proper, from a highly compact state at low urea concentrations to a more significantly expanded state at higher denaturant concentrations (*17*). This raises concerns about the meaning of $\Delta G^{o}_{urea}$, $\Delta G^{o}_{Gdn}$, and $\Delta G^{o}_{T}$ (*17*). For proteins that denature with variable two-state behavior, the denatured ensemble in the limit of zero denaturant concentration need not be related structurally or thermodynamically to the denatured ensemble during the actual denaturational transition (*17*). Treatment of systems that exhibit variable two-state character in terms of a fixed two-state model might not be appropriate, and the physical meaning of $\Delta G^{o}$ values obtained by extrapolation in these cases is not clear. None of the experimental data in the present study address this aspect of the validity of $\Delta G^{o}_{urea}$ and $\Delta G^{o}_{T}$ directly. However, as discussed ahead, the peculiar pH dependence of stability reported by $\Delta G^{o}_{urea}$ and $\Delta G^{o}_{T}$ is actually consistent with the behavior expected if the D state were compact. We interpret the agreement between $\Delta G^{o}_{urea}$ and $\Delta G^{o}_{T}$ over the wide range of pH studied as evidence that the changes in the thermodynamic character of the denatured ensemble during the denaturational transition

proper do not bias the measured $\Delta G°$ significantly. The physical basis of the denaturing action of urea and heat are very different, and there is no reason to expect the denaturant-induced changes in the D state during the urea and heat-induced transitions to be the same.

*Electrostatic Interactions in the Denatured State.* The pH dependence of stability described by $\Delta G^{o}_{\Delta\nu}$ is very steep. $\Delta G^{o}_{\Delta\nu}$ represents the free energy difference between the N and U states, and its pH dependence reflects large differences between the p$K_a$ values of ionizable groups in these two states. In the U state, all p$K_a$ values converged to the values of model compounds, partly because this state is expanded and unstructured, and also because charged groups are highly screened in the high ionic strength of 6 M GdnHCl. The destabilization of the N state relative to the U state between pH 9 and 5 shows that p$K_a$ values of histidines and of acidic residues are, on average, considerably lower in N than in U.

In contrast to the steep pH dependence of $\Delta G^{o}_{\Delta\nu}$, the stability of N relative to the D state described by $\Delta G^{o}_{urea}$ and $\Delta G^{o}_{T}$ is less sensitive to pH between pH 9 and 5. The presence of some histidines and maybe even some acidic groups that titrate with nativelike, depressed p$K_a$ values in the D state needs to be invoked to rationalize the shallower pH dependence of $\Delta G^{o}_{urea}$ and $\Delta G^{o}_{T}$. Note that this conclusion could have been reached in the absence of the $H^+$ titration curves measured in GdnHCl. Knowledge of the $H^+$ titration behavior of the N state (Figure 1, panel A) and of p$K_a$ values of model compounds in water and in GdnHCl alone, would have been sufficient to establish that the p$K_a$ values of some groups in the D state are nativelike and perturbed relative to the values of model compounds. Use of the term "nativelike" to describe p$K_a$ values of histidines in the D state is only meant to emphasize that the p$K_a$ values are depressed and not that the microenvironments of these residues in N and D states are comparable.

The nativelike $H^+$ binding properties of the D state were evident in earlier DSC studies of the pH dependence of thermal unfolding of wild-type SNase, although that was not the interpretation given to those data (*18*). The number of $H^+$ that were bound upon thermal denaturation over a range of pH values was lower than the number expected to be bound by the D state if the ionizable groups in this state titrated with the p$K_a$ values of model compounds. For example, whereas the data in Figure 1, panel B, show that at pH 7 nearly 1.5 $H^+$ are bound preferentially by U relative to N, the DSC experiments (*18*) showed that only 0.1 $H^+$ were bound upon thermal unfolding at this pH. Even at pH values close to $pH_{mid}$, where the data in Figure 1, panel B, show that nearly 5 $H^+$ are bound upon unfolding to the U state, the number of $H^+$ bound upon thermal unfolding was only 0.7. The DSC data show that the transition between the native and the heat-denatured state proceeds without normalization of p$K_a$ values, consistent with a transition between the native and a very compact denatured state with nativelike and substantially depressed p$K_a$ values.

The pH dependence of stability of SNase between pH 9 and pH 5 is probably determined by the five groups most likely to titrate in this pH range: His-8, His-46, His-121, His-124, and the N-terminus. The N-terminus is disorganized in the crystal structure. It is probably safe to assume that its p$K_a$ is the same in native and non-native states. The p$K_a$ values of the four histidines were determined by Markley and co-workers (*39*). The measurements were performed at an ionic strength of 0.3 M, higher than the 0.1 M ionic strength in the urea and heat denaturation experiments. The p$K_a$ values are His-8, 6.8; His-46, 5.8; His-124, 6.0; His-121, 5.5. Three of the four histidines have p$K_a$ values lower than the model compound value of 6.3. This is consistent with the behavior described in Figure 1, panel B. The depressed p$K_a$ values of His-46, His-121, and His-124 in the N state can account for the 3.7 kcal/mol difference in $\Delta G^{o}_{\Delta\nu}$ between pH 5 to pH 9.

The molecular determinants of p$K_a$ values in the N state are currently under study with H NMR spectroscopy and structure-based computational methods in our laboratory. One goal is to determine why in SNase the p$K_a$ values of many groups that ionize below pH 9 are depressed. The p$K_a$ values of histidines can be depressed either by loss of solvation or through repulsive electrostatic interactions. Visual inspection of the crystallographic structures of SNase did not reveal any obvious molecular reasons for the depressed p$K_a$ values of His-46, His-121, and His-124. His-46 is in a loop that is one of the most disordered regions of the protein. Both N$\epsilon$ and N$\delta$ nitrogen atoms of the imidazole group are solvent-accessible, and there are no charge bearing atoms in the immediate vicinity. The same is true for His-121 and His-124. These two histidines are located at the beginning of the C-terminal helix, purportedly the least stable element of secondary structure, the last one to assemble, and the one most likely to unfold (*19*). They are neither buried nor in direct contact with the charged moieties of other basic groups. However, SNase is a highly basic protein, with pI > 10. Twenty three lysines and five arginines bear positive charge below this pH. We believe that the depressed p$K_a$ values of histidines and of acidic residues in the N and in the D states reflect medium to long-range interactions with the constellation of Lys and Arg residues on the surface of the protein.

Compactness in the D state needs to be invoked to rationalize the depressed p$K_a$ values in this state in terms of the very high background of positive charge. For two reasons, we deem it unlikely that the depressed p$K_a$ values of the histidines could be explained in terms of interactions with other basic groups nearby in the primary sequence, as they might occur in an extended unfolded state. First, only His-8 and His-46 have neighboring basic groups in sequence; His-121 and His-124 have none. Second, the p$K_a$ of a histidine embedded in a pentapeptide with a net charge of +2, similar to the case of His-8 and His-46, was 6.5 in 300 mM ionic strength (*35*). This suggests that even if the segments surrounding the histidines were unstructured, repulsive interactions between basic groups that are neighbors in sequence could not account for the depressed p$K_a$ values of histidines in the D state of SNase. In the compact D state, the distances between charged atoms would presumably be small enough for electrostatic interactions to be significant. In this sense, the presence of substantial electrostatic interactions in the D state is consistent with the structured and compact character of this state deduced by the extensive NMR and mutagenic studies by Shortle and co-workers (*16*, *19*) and more directly by measurements of hydrodynamic radii of the denatured ensemble (*15*, *17*).

The stability curves in Figure 5, panel A, constitute a map of the pH dependence of the Gibbs free energy differences between N, D, and U states of SNase. According to these data, the stability of the D state relative to U is significantly pH-sensitive. Note that while the free energy distance between N and U in the region near pH 5 and pH 4 is still twice that between N to D, the two stability curves converge as the pH nears the pH where acid denaturation was observed. At pH < 4.5, the difference in free energy distance between D and U is close to thermal energy. As noted earlier, the $H^+$ binding properties of the $U_A$ state and of the U state are very similar (Figure 1, panel B). By extension, there are substantial differences in the $H^+$ binding properties of the $U_A$ states achieved in acid and the D state achieved in urea or with heat at pH > 5. However, in terms of their $H^+$ titration properties, the D state that is populated at pH < 5 begins to resemble the $U_A$ state. Acid denaturation would not occur unless there were substantial differences in the p$K_a$ values of acidic residues in N and $U_A$ states. At pH < 5, the character of the D state changes toward a state in which Glu and Asp residues titrate with p$K_a$ similar to those of model compounds, and this is the source of the steep decrease in $\Delta G^o_{urea}$ and $\Delta G^o_T$ below pH 5.

The idea that the thermodynamic properties of the D state change at pH < 5 is consistent with the structural interpretation given by Pace and co-workers to the increase in *m* values with decreasing pH found for several proteins (*11*, *12*). This dependence of *m* values on pH has been interpreted in terms of an expansion of the D state driven by the repulsive interactions that accrue concomitant with neutralization of acidic residues (*11*, *12*). It has been pointed out previously that the *m* value of denaturation of SNase reflects factors other than the amount of surface area that is exposed to solvent upon denaturation (*17*). Note, however, that the pH dependence of the *m* values of urea denaturation of SNase follow the trend observed for other proteins (Figure 5, panel B). *m* values increase from 2.28 kcal $mol^{-1}$ $M^{-1}$ at pH 9, to 4.15 kcal $mol^{-1}$ $M^{-1}$ near $pH_{mid}$. The increase in *m* values with decreasing pH mirrors the pH dependence of $\Delta G^o_{urea}$. The increase in *m* values at pH ≤ 5 correlates with a shift in the thermodynamic properties of the D state toward a state in which the p$K_a$ values of acidic residues are normalized. Normalization of p$K_a$ values implies a loss of electrostatic interactions between acidic and basic residues, which would be the expected consequence of an expansion of the D state.

In all previous studies of electrostatic interactions in D states, the interactions that were detected were, on average, stabilizing (i.e., depressed p$K_a$ values of acidic residues). In contrast, in the case of SNase the electrostatic interactions in the D state evidenced by the differences in the pH dependence of $\Delta G^o_{\Delta\nu}$ and of $\Delta G^o_{urea}$ and $\Delta G^o_T$ in the pH range 4.5 to 9 are primarily the repulsive interactions between histidines and the other basic residues. The presence of these repulsive interactions suggests that despite the greater plasticity and conformational pliability of the D state as compared to the N state, it is not free to relieve these repulsions through a conformational transition. The electrostatic interactions responsible for the pH dependence of stability in the pH range 4.5 to 9 are a consequence rather than a cause of compactness. Presumably, the D state remains compact despite these repulsive forces because of compensation by favorable electrostatic interactions between acidic and basic groups, which favor compactness, or by other types of noncovalent interactions that also favor the compact state and which are only disrupted when high $H^+$ concentrations shift the equilibrium between conformational states in favor of a D state with higher $H^+$ affinity (i.e., a D state in which the p$K_a$ values of acidic residues are normalized). On the basis of the demonstrated urea-dependence of the dimensions of the D state at pH 7 (*17*), it is likely that before it expands near pH 5, the D state actually contracts as the pH drops from 9 to 5 because acidification lowers the concentration of urea needed to denature the protein (*17*).

Electrostatic interactions cannot contribute to the stability of the N state of proteins when the electrostatic interactions in the D state are similar to those of the N state. However, the modulation of compactness of the D state through electrostatic interactions could have important implications for the stability of thermostable proteins at high temperatures. The dielectric constant of water decreases with increasing temperature; therefore, electrostatic interactions become stronger at high temperatures. If the D state were pliable, strengthening of the electrostatic interactions could in turn alter the amount of surface area exposed to water during the transition from N to D. This could affect $\Delta C_p$ and consequently also the temperature dependence of $\Delta G°$. Proteins from thermophilic organisms are known to have a higher number of charged residues than their mesophilic counterparts. Most discussions on the significance of the higher charge density of thermophilic proteins have focused on putative contributions by ion pairs to the stability of the N state. The findings of this study suggest that the electrostatic contributions to thermostability could operate at the level of the denatured ensemble.

## SUMMARY

The significance and implications of these thermodynamic studies are the following. First, the pH dependence of stability of the D state relative to the U state where all electrostatic effects are annulled was obtained by comparing the free energy difference between N and D states measured by fluorescence-monitored denaturation with the free energy difference between N and U states calculated by numerical integration of $H^+$ titration curves. Second, the difference in the pH dependence of stability obtained with two different equilibrium thermodynamic methods was interpreted as evidence of substantial electrostatic interactions in the D state, thought to result from its high charge density coupled to its compact character. The data at hand are not sufficient to explain how electrostatic interactions influence the structure and compactness of the D state. Third, these studies provide significant insight about the magnitude of electrostatic interactions in the N state. These interactions are actually quite substantial, but they are also strong in the D state, thus the apparent lack of a significant contribution by electrostatics to the stability of SNase. The data suggest that in an earlier study, the inability to rationalize the effects of mutations of ionizable groups in SNase stemmed partly from the invalid assumption that all electrostatic effects are annulled in the D state (*42*). Fourth, in this study we have demonstrated how the thermodynamic character of the compact D state of SNase can be accessed through the study of proton-linked stability and $H^+$ titration curves. The

experimental approach outlined in this study will be useful to study the molecular determinants of compactness. Finally, one of the reasons that site-directed mutagenesis has not lived up to its promise as a tool to explore quantitatively the contributions by specific residues or noncovalent interactions to the structure, folding, and stability of proteins is that the effects of mutations on conformation and on thermodynamic properties cannot be assessed independently for the N and D states. The ability to reference the stability of both N and D states of SNase relative to the U state, a state whose thermodynamic character can be accessed by measurement of its $H^+$ binding properties, will improve our ability to rationalize the effects of mutations in terms of structural and thermodynamic consequences in both native and denatured states.

## ACKNOWLEDGMENT

We thank Prof. David Shortle (Johns Hopkins University School of Medicine) for his gift of overproducing strains. Technical advice and critical comments by David Shortle and Wayne Bolen (University of Texas Medical Branch) are also gratefully acknowledged.

## REFERENCES

1. Schaefer, M., Van Vlijmen, H. W. T., and Karplus, M. (1998) *Adv. Protein Chem. 51*, 1.
2. Tanford, C. (1969) *Adv. Protein Chem. 24*, 1.
3. Tanford, C. (1962) *Adv. Protein Chem. 17*, 69.
4. Matthew, J. B., Gurd, F. R. N., García-Moreno E., B., Flanagan, M. A., March, K. L., and Shire, S. J. (1985) *CRC Crit. Rev. Biochem. 18*, 91.
5. Oliveberg, M., Vuilleumier, S., and Fersht, A. R. (1994) *Biochemistry 33*, 8826.
6. Oliveberg, M., Arcus, V. L., and Fersht, A. R. (1995) *Biochemistry 34*, 9424.
7. Tan, Y., Oliveberg, M., Davis, B., and Fersht, A. F. (1995) *J. Mol. Biol. 254*, 980.
8. Barrick, D., and Baldwin, R. L. (1993) *Biochemistry 32*, 3790.
9. Ionescu, R. M., and Eftink, M. R. (1997) *Biochemistry 36*, 1129.
10. Barrick, D., Hughson, F. M., and Baldwin, R. L. (1994) *J. Mol. Biol. 237*, 588.
11. Pace, C. N., Laurents, D. V., and Thomson, J. A. (1990) *Biochemistry 29*, 2564.
12. Pace, C. N., Laurents, D. V., and Erickson, R. E. (1992) *Biochemistry 31*, 2728.
13. Swint-Kruse, L., and Robertson, A. D. (1995) *Biochemistry 34*, 4724.
14. Kuhlman, B., Luisi, D. L., Young, P., and Raleigh, D. P. (1999) *Biochemistry 38*, 4896.
15. Eftink, M. R., and Ramsay, G. D. (1997) *Proteins: Struct., Funct. Genet. 28*, 227.
16. Shortle, D. (1995) *Adv. Protein Chem. 45*, 217.
17. Baskakov, I. V., and Bolen, D. W. (1998) *Biochemistry 37*, 18010.
18. Carra, J. H., Anderson, E. A., and Privalov, P. L. (1994) *Protein Sci. 3*, 944.
19. Wang, Y., and Shortle, D. (1995) *Biochemistry 34*, 15895.
20. Bolen, D. W., and Santoro, M. M. (1988) *Biochemistry 27*, 8069.
21. Yao, M., and Bolen, D. W. (1995) *Biochemistry 34*, 3771.
22. Shortle, D., and Meeker, A. K. (1989) *Biochemistry 28*, 936.
23. Flanagan, M. A., García-Moreno E., B., Friend, S. H., Feldmann, R. J., Scouloudi, H., and Gurd, F. R. N. (1983) *Biochemistry 22*, 6027.
24. Johnson, M., and Frasier, S. (1985) *Methods Enzymol. 117*, 301.
25. García-Moreno E., B., Dwyer, J. J., Gittis, A. G., Lattman, E. E., Spencer, D. S., and Stites, W. E. (1997) *Biophys. Chem. 64*, 211.
26. Shortle, D., Meeker, A. K., and Freire, E. (1988) *Biochemistry 27*, 4761−4768.
27. Carra, J. H., Anderson, E. A., and Privalov, P. L. (1994) *Protein Sci. 3*, 952.
28. Carra, J. H., Anderson, E. A., and Privalov, P. L. (1994) *Biochemistry 33*, 10842−10850.
29. Chen, H. M., and Tsong, T. Y. (1994) *Biophys. Chem. 66*, 40−45.
30. Chen. H. M., You, J. L., Markin, V. S., and Tsong, T. Y. (1991) *J. Mol. Biol. 220*, 771−778.
31. Epstein, H. F., Schechter, A. N., Chen, R. F., and Anfinsen, C. B. (1971) *J. Mol. Biol. 60*, 499.
32. Roxby, R., and Tanford, C. (1971) *Biochemistry 10*, 3348.
33. Nozaki, Y., and Tanford, C. (1967) *J. Am. Chem. Soc. 89*, 736.
34. Nozaki, Y., and Tanford, C. (1967) *J. Am. Chem. Soc. 89*, 742.
35. Kao, Y., Fitch, C. A., Bhattacharya, S., Sarkisian, C. J., Lecomte, J. T. J., and Garcia-Moreno E., B. (2000) *Biophys. J. 79*, 1637.
36. Yang, M., Liu, D., and Bolen, D. W. (1999) *Biochemistry 38*, 11216.
37. Fink, A. L., Calciano, L. J., Goto, Y., Nishimura, M. and Swedberg, S. A. (1993) *Protein Sci. 2*, 1155.
38. Wrable, J. (1999) Ph.D. dissertation, Johns Hopkins University.
39. Alexandrescu, A. T., Mills, D. A., Ulrich, E. L., Chinami, M., and Markley, J. L. (1988) *Biochemistry 27*, 2158.
40. Antosiewicz, J., McCammon, J. A. K., and Gilson, M. K. (1994) *J. Mol. Biol. 238*, 415−36.
41. Yang, A.-S., and Honig, B. (1993) *J. Mol. Biol. 231*, 459−474.
42. Meeker, A. K., García-Moreno E., B., and Shortle, D. (1996) *Biochemistry 35*, 6443−6449.

BI001015C